Color symmetry and altermagneticlike spin textures in noncollinear antiferromagnets

Paolo G. Radaelli[*]
Clarendon Laboratory, Department of Physics, University of Oxford, Oxford OX1 3PU, United Kingdom

Gautam Gurung[†]
Trinity College, University of Oxford, Oxford OX1 3BH, United Kingdom

(Received 14 January 2025; revised 28 May 2025; accepted 12 June 2025; published 17 July 2025)

We present a formalism based on color symmetry to analyze the momentum-space spin textures of noncollinear antiferromagnets. We show that, out of the spin textures allowed by the magnetic point group, one can extract a component that is invariant by general rotations in spin space, and can exist in the absence of spin-orbit coupling, in complete analogy to spin textures in altermagnets. We demonstrate this approach in the case of three complex, noncollinear magnets, $Mn_3Ir(Ge,Si)$, Pb_2MnO_4, and Mn_3GaN. For Mn_3GaN, we also show that the predictions of color-symmetry analysis are consistent with density functional theory calculations performed on the same system both with and without spin-orbit coupling.

DOI: 10.1103/r34k-xjpx

I. INTRODUCTION

In the past five years, an intense theoretical and experimental effort has been focused on magnetic systems having electronic bands with lifted spin degeneracy, particularly when this is not due to spin-orbit coupling (SOC) (for example, Refs. [1,2]; see Ref. [3] for a full list of references). Collinear magnets with symmetry-driven compensated net magnetization displaying this phenomenology have been named "altermagnets," though this term has been applied by others to a wider group of systems that display spin splitting in momentum space; see for example Ref. [4]. Three broad classes of magnetic materials are often included in this extended classification: altermagnets *stricto sensu*; noncollinear compensated antiferromagnets that, like altermagnets, have spin splitting that is $\mathbf{k}/-\mathbf{k}$ *symmetric* and time-reversal odd (TRO); and other systems, including so-called *p*-wave magnets [5] and triangular magnetic lattices [6], in which spin splitting is $\mathbf{k}/-\mathbf{k}$ *antisymmetric* and time-reversal even (TRE) [7]. In analogy with the celebrated Rashba-Dresselhaus (R-D) effect [8,9], the latter require inversion-symmetry breaking, but unlike R-D systems, do not require SOC. In a previous paper [3], one of us (P.G.R.) presented a symmetry classification of $\mathbf{k}/-\mathbf{k}$-symmetric, TRO splitting of electronic bands in magnetic materials based on a general tensorial approach and with a focus on (collinear) altermagnets. It was also shown that, for collinear compensated magnets where the splitting is allowed (i.e., those whose symmetries do not contain the time-reversal operator or the product of inversion and time-reversal operators), one can decompose the spin texture into two components: a SOC-independent "altermagnetic" texture, having a general form that can be obtained via the spin group (SG) analysis (or an analog based on black-and-white Shubnikov groups), and a "residual" component, which is allowed by the exact magnetic point group (MPG) symmetry for a particular direction of the Néel vector and will only exist in the presence of SOC.

The existence of nonrelativistic spin textures in *noncollinear* antiferromagnets was discussed before altermagnetism emerged as a distinct concept [10], while spin-dependent density functional theory (DFT) calculations on noncollinear magnets have been performed as far back as 1989 [11]. Collinear and noncollinear magnets can possess the same MPG symmetries (though cubic MPG can only describe noncollinear magnets), and there is general consensus that the SG analysis, with some modifications, can be extended to noncollinear systems. Nevertheless, no systematic methods have been proposed to date to extract SOC-independent textures in noncollinear systems. Here, we fill this gap by employing a systematic approach based on so-called color symmetry groups (CGs) to describe $\mathbf{k}/-\mathbf{k}$-*symmetric*, time-reversal odd altermagneticlike textures in collinear and noncollinear magnets [12]. In Ref. [3], it was shown that Shubnikov groups offer an alternative formulation of the SG analysis and offer some advantages; for instance, they preserve the natural concept of time-reversal symmetry. The CGs we employ here are a natural extension of black-and-white Shubnikov groups to cases in which there are more than two spin directions. Although CGs and SGs are largely equivalent and can both be employed to describe noncollinear SOC-independent textures, CGs are more intuitive and do not require the rather cumbersome choice of the SG axis orientation. We will demonstrate the application of this CG analysis to three noncollinear

[*]Contact author: p.g.radaelli@physics.ox.ac.uk
[†]Contact author: gautam.gurung@trinity.ox.ac.uk

chiral magnets: $Mn_3Ir(Ge,Si)$, Pb_2MnO_4, and Mn_3GaN. The magnetic structures of $Mn_3Ir(Ge,Si)$ and Pb_2MnO_4 are described by complex four-color symmetries, but do not break any crystal symmetries, which means that the CG and MPG analyses are expected to (and do) yield the same textures. Finally, for the well-known noncollinear magnetic antiperovskite Mn_3GaN, we present the CG analysis, including a full tensorial decomposition, alongside spin-resolved DFT calculations with and without SOC. In complete analogy with the case of collinear altermagnets, we show that, in the absence of SOC, the spin texture is exactly as predicted by the CG analysis, while in the presence of SOC, an additional component emerges, which has the more general MPG symmetry and varies depending on the direction of the magnetic moments.

II. ALTERMAGNETISM AND SPIN-SPACE ROTATION INVARIANCE

The intuitive statement that the SOC-independent component of the spin texture (the altermagnetic component in collinear systems) is invariant by rotation in spin space requires some qualification. In $\mathbf{k}/-\mathbf{k}$-*symmetric* TRO altermagnets, the spin texture can be thought of as generated by an effective Zeeman field $\mathbf{B}^{eff}(\mathbf{k}, n)$, which depends on the wave vector k and on the band index n [3]. More rigorously, within the context of DFT, for a given wave vector $\mathbf{k}$ and band index n the spin texture is defined by the vector field $\mathbf{s}_{n\mathbf{k}} = \langle\Psi_{n\mathbf{k}}|\,\boldsymbol{\sigma}\,|\Psi_{n\mathbf{k}}\rangle$, where $\boldsymbol{\sigma}$ is a vector of Pauli matrices and the integral implied by the $\langle\ |$ and $|\ \rangle$ is over the real-space unit cell. Although the two fields, though different in magnitude, are equivalent from the symmetry point of view, in this paper we will employ $\mathbf{s}_{n\mathbf{k}}$ to make a direct connection with our DFT results (see below). Within the tensorial framework, to a given order the spin textures can be expressed as

$$\mathbf{s}_{n\mathbf{k}} = T^{(l)}_{i,\alpha\beta\gamma\ldots} k_\alpha k_\beta k_\gamma \ldots, \tag{1}$$

where $T^{(l)}_{i,\alpha\beta\gamma\ldots}$ is a tensor of odd rank that is symmetric in the Greek indices.

If $\mathbf{s}_{n\mathbf{k}}$ is generated by a collection of real-space magnetic moments $\mathbf{S}_j$ within the crystal structure, "rotational invariance in spin space" means that, upon a global spin-space rotation of the $\mathbf{S}_j$'s, the *amplitude* $|\mathbf{s}_{n\mathbf{k}}|$ is invariant, while the vector field direction corotates with the $\mathbf{S}_j$'s. Mathematically, this can be expressed as

$$\mathbf{s}_{n\mathbf{k}}(\mathbf{S}_j) = \boldsymbol{R}^{-1}\mathbf{s}_{n\mathbf{k}}(\boldsymbol{R}\,\mathbf{S}_j), \tag{2}$$

where $\boldsymbol{R}$ is any rotation matrix. For collinear magnetic structures, one can verify that the SG construction produces an $\mathbf{s}_{n\mathbf{k}}$ with the invariance properties of Eq. (2). Again, this is most easily seen using the equivalent Shubnikov approach: the SG-equivalent Shubnikov group is the symmetry group of the black-and-white antiferromagnetic ordering pattern, and is therefore independent on the direction of the Néel vector. As discussed in Ref. [3], one proceeds to construct a *scalar* field $s_{n\mathbf{k}}$ from a tensor that is fully symmetrized by the Shubnikov SG, and then equates $\mathbf{s}_{n\mathbf{k}} = \hat{\mathbf{L}}\, s_{n\mathbf{k}}$, where $\hat{\mathbf{L}}$ is a unit vector in the direction of the Néel vector $\mathbf{L}$. Since in a collinear structure $\mathbf{L}$ and the $\mathbf{S}_j$ are both parallel/antiparallel to each other, Eq. (2) is obeyed by construction. Our aim is to find an analogous treatment for $\mathbf{k}/-\mathbf{k}$-symmetric, TRO textures in *noncollinear* magnets, so that $\mathbf{s}_{n\mathbf{k}}$ is similarly invariant by construction. Note that this approach is not immediately suitable for $\mathbf{k}/-\mathbf{k}$-antisymmetric magnets, since in this case the spin texture cannot be described as a linear combination of TRO vectors with scalar quantities, which clearly produces a TRO, parity-even tensor. Moreover, in $\mathbf{k}/-\mathbf{k}$-antisymmetric magnets, band splitting and spin polarization are correlated, so that, for a given k, the net spin polarization averaged over bands that would be degenerate in the absence of magnetic ordering is zero [13].

III. COLOR SYMMETRY GROUPS AND THE DESCRIPTION OF NONCOLLINEAR STRUCTURES

Color symmetry groups are groups of combined geometrical and color-permutational symmetry operations, which leave certain colored objects unchanged [14]. In the context of crystallography, one can distinguish between color *point* groups (CPGs), where all geometrical transformations are proper and improper rotations around a fixed point, and color *space* groups (CSGs), in which rotations and translations are combined to yield the symmetries of periodic colored objects. Within the CG framework, Shubnikov groups correspond to *bicolor* CGs. Tricolor CSGs were first classified by Harker in 1981 [14], while other authors later extended the theory to four and six colors [15–17]. A full classification of all possible CSGs was presented by Kozev in 1988 [18]. Applications of CGs to physical problems were discussed as early as 1982 [19] and were later extended to include the description of orbital ordering [20]. Although extending the Shubnikov group analysis of magnetic structures to multicolored groups appears quite natural, by the early 1980s the representation analysis first introduced by Bertaut [21] was already very popular, and the alternative CSG approach was not widely pursued.

Here, we will adopt the nomenclature first proposed by Harker to construct multicolor groups [14], in which each CSG/CPG is denoted by an ordinary space or point group, say G, followed by two of its subgroups, H and H'. H' is a subgroup of index n, where n is also the number of colors, and contains all the operations in G that leave one color invariant, so that, for example, "red" fragments are transformed in other red fragments. Other colors are left invariant by conjugated copies of H', which are not necessarily unique to a single color. By contrast, H contains all the operations in G that leave *all* colors invariants. Strictly speaking, adding H to the notation is redundant, because H is the intersection of H' with all its conjugated subsets and can be readily obtained from H' and G. Note also that the color permutation group is isomorphic to the quotient group G/H. Within this framework, the color symmetry of a particular structure would consist of an ordinary point or space group operation, which only affects the position of the atoms (or fragments), composed with ($\circ$) a color-permutation operation, which only affects the colors. So, for example, if a certain geometrical operation g converts red (R) fragments to red fragments and exchanges blue (B) and green (G) fragments, the corresponding CG operation is $g \circ \{R \to R, B \to G, G \to B\}$.

When using CGs to describe magnetic structures, each direction of the magnetic moments would be represented by a distinct color. It seems useful to consider time reversal as a special operation (denoted as $1'$), so that structural fragments containing spins related by time reversal are represented by "anticolors" (e.g., red and antired spins would be opposite and related by time reversal). Using the notation above, $1' \equiv \{R \to \bar{R}, B \to \bar{B}, G \to \bar{G}\}$, where the bar indicates the anticolor. An advantage of this approach is that, at any tensor rank, it is possible to represent a color/anticolor pair with the same colored tensor, as explained further in Sec. IV. Moreover, the notion of time reversal is preserved, as in the case of Shubnikov groups.

The exact symmetry group of the crystal + magnetic structure (MPG or magnetic space group, MSG) consists of all CPG/CSG operations for which the color permutation corresponds to a geometrical axial vector transformation combined either with the identity or with time reversal. Hence, the MPG/MSG of a given magnetic structure is a subgroup of its CPG/CSG. By construction, magnetic structures related by a global rotation in spin space are described by the same CG, the only difference being the identification of colors with spins.

Ever since the work of Bertaut [21], irreducible representations of space groups have been the primary tool to describe magnetic structures. Later, Izyumov introduced exchange multiplets, which are sets of irreducible representations that are linked together if the magnetic Hamiltonian is invariant by rotations in spin space. There is a natural link between CGs and the theory of exchange multiplets [22], which is discussed in the Appendix.

A. Color group notation

Following Harker [14], the CG notation used in the remainder of this paper is $\{G|H'|H\}$. Although this notation is rather verbose and may be conveniently simplified if the use of color groups were to become widespread, it has the merit of being complete and accurate and of using only familiar crystallographic symbols.

For example, in the case of Mn_3GaN (see below), the parent crystallographic group is $G = 4\bar{3}m$, the subgroup H' that leaves one color invariant is $4/mmm$, and the intersection of the three conjugated H' groups is the group $H = mmm$. Hence, the notation for the corresponding 3-color group is $\{4\bar{3}m|4/mmm|mmm\}$. If the parent group G is centrosymmetric, one can simplify calculations significantly by dropping all improper operators. In this case, the corresponding color group is $\{432|422|222\}$.

The notation for the other two systems discussed in this paper [$Mn_3Ir(Ge,Si)$ and Pb_2MnO_4] is obtained in the same way. In the simplified 4-color description of $Mn_3Ir(Ge,Si)$, each color is left invariant by a 3-fold axis, so the H' group is 3, leading to the notation $\{23|3|1\}$ (only the identity operator leaves all colors invariant). In the 12-color scheme, no color is left invariant by operators other than the identity, so the color group notation is $\{23|1|1\}$. In the case of Pb_2MnO_4, the parent group is $\bar{4}2m$, while the H' subgroup is m, with no intersection between the H' groups for different colors other than the identity. Therefore, the color group notation is $\{\bar{4}2m|m|1\}$.

B. Color groups and spin groups

Since each crystallographic point group (XPG) is isomorphic to a permutation group, it is not surprising that a close relation exists between the CG and SG analyses of both collinear and noncollinear magnetic structures. This relation becomes transparent if one assigns a distinct color to each arm of the star generated by the part of the SG that acts exclusively on spins, since the action of the SG on spins becomes equivalent to a color permutation. The derivation of all SGs [23] is largely identical to that of CPGs; for example, in Ref. [23], the groups G and H are called R and r. However, in the SG derivation, there is an extra step to associate with the quotient group R/r one of the 32 XPGs (called B in Ref. [23]). It should also be noted that CG symbols encode extra information with respect to SGs. This includes not only the number of colors (i.e., of distinct spin directions), but also the specific representation of the symmetry groups that defines the transformation of all magnetic structures with the same CG symmetry (this is explained in more detail in the Appendix). In the case of SGs, the same information is encoded in the orientation of the magnetic moments with respect to the symmetry operators of the group B. This will be further clarified in the examples given below.

The general group-theoretical statement connecting MPGs, SGs, and CGs is that, for a given magnetic structure, the MPG that describes it is a subgroup of the SG, which is itself a subgroup of the CG, though these are not necessarily *proper* subgroups (in other words, pairs of these groups may be isomorphic). In many cases of interest (including all those discussed in this paper), SGs and the corresponding CGs are also isomorphic, so whether one uses CG or SG is largely a matter of preference. However, this is not always the case. Typically, CG and SG are nonisomorphic when spins connected by color (permutation) operations do not have the same magnitude, generally as a consequence of a magnetic phase transition that splits equivalent sites into inequivalent "orbits." An example of this is discussed in the Supplemental Material (SM) [37], Sec. I. When the CG is a proper supergroup of the SG, the CG analysis is more general and may unveil "hidden" symmetries that are invisible to the SG analysis.

We also find the CG approach to be somewhat more intuitive: In the case of SG and for a generic orientation of the magnetic moments (e.g., in the presence of an applied magnetic field), the point group elements acting on spins are generally not coaligned with those acting on atoms, and their operators do not coincide with any of the symmetry operators that are present in the paramagnetic structure. By contrast, spin (or color) permutation has the same meaning regardless of the overall spin orientation. An example of parallel SG and CPG analyses will be given in Sec. VII B.

IV. CONSTRUCTING COLORED ALTERMAGNETIC TENSORS

The procedure to construct altermagnetic tensors in the framework of CG theory is rather straightforward, and follows closely the case of collinear structures (bicolor groups). Using the projection method, one constructs sets of *colored tensors* that are totally symmetric by the CPG of the magnetic

structure. This is done beginning with the most generic form of a symmetric tensor of a given rank, and assigning to it a single color (say, red). The "red" tensor is then constructed by adding up all copies of the original tensor transformed in the usual way via symmetry operations in H', where H' transforms red fragments into other red fragments, and normalizing by the order of G. Likewise, the "blue" tensor is obtained by adding up all copies of the original tensor transformed via $g \circ H'$, where g transforms red fragments into blue fragments, etc. The full altermagnetic tensor is then obtained as a linear combination of the colored tensors *times* the axial unit vector corresponding to the color assigned to the magnetic moment in the real-space structure. Once again, by construction, effective magnetic fields (i.e., spin textures) calculated using this method are invariant by Eq. (2), since magnetic moments in real space and axial unit vectors in reciprocal space are parallel and hence corotating. Moreover, since the MPG of the magnetic structure is a *subgroup* of the CPG, it follows that the altermagnetic tensor thus constructed is always a *special case* of the general MPG tensor, which can then be decomposed into "altermagneticlike" and residual components, precisely as in the collinear case.

The procedure to obtain colored tensors is slightly modified in the presence of geometrical operators composed with the time-reversal operator $1'$, which gives rise to anticolors. One can obtain separate tensors for a given color (say, red) and its anticolor (antired). However, when the full tensor is reconstructed, the red and antired tensors will be multiplied by antiparallel vectors, which is equivalent to multiplying the "red" vector by the *difference* of the two tensors. Using this method, one effectively halves the number of required tensors. This mirrors the procedure outlined in Ref. [3] for collinear structures, where only one TRO tensor was required rather than separate "black" and "white" tensors. This situation is discussed further in Sec. VI.

V. Mn_3Ir(Ge, Si)

Mn_3Ir(Ge,Si) crystallizes in the crystallographic space group $P2_13$. Below the Néel temperature ($T_N = 225$ K for Ge and 210 K for Si), magnetic moments on the 12 magnetic sites order forming a complex noncollinear structure with the MSG also being $P2_13$ (MPG 23) [24,25]. Spin textures and bulk properties in Mn_3IrSi were recently analyzed theoretically and discussed in the context of Landau theory [26].

In the magnetic structure refined from experimental data and also confirmed by theoretical calculations [24,25], all the magnetic moments on the 12 sites are noncollinear, so analyzing the magnetic structure with CG-SG would require 12 colors or 12 distinct spin-space rotations. However, groups of three moments are roughly parallel to each other and to one of the cube diagonals, the angle with the closest diagonal being $\sim 11^\circ$. The experimental magnetic structure (a) and the approximate structure (b) are displayed in Fig. 1. We begin by performing an analysis of the spin textures for the approximate structure, which requires four colors. Later, we will explain that the 12-color analysis yields an identical result. Since the magnetic and crystallographic space groups are the same, the magnetic structure does not break any crystallographic symmetry. We therefore expect the textures arising from the 4- and 12-color analyses to be fully consistent with the MPG textures, which are reported in Table I of Ref. [3] (MPG 23, Class XVII).

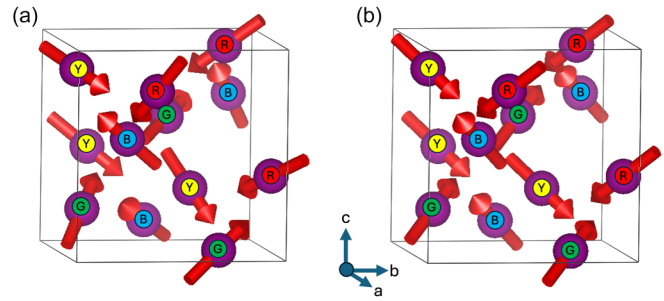

FIG. 1. Experimentally determined [24] (a) and approximate (b) magnetic structures of Mn_3Ir(Ge,Si). Only magnetic Mn atoms are shown. Labels indicate distinct colors (see text for the assignment of magnetic moment directions to colors).

A. Mn_3Ir(Ge, Si): Four-color analysis

We choose the four colors to correspond to the following spin directions [see Fig. 1(b)]:

$$\begin{aligned} \text{Yellow (Y)} &: \rightarrow (1, 1, -1), \\ \text{Blue (B)} &: \rightarrow (1, -1, 1), \\ \text{Green (G)} &: \rightarrow (-1, 1, 1), \\ \text{Red (R)} &: \rightarrow (-1, -1, -1). \end{aligned} \tag{3}$$

The XPG (23) comprises 12 symmetry operations: eight 3-fold ($\pm 120^\circ$) rotations, around [1,1,1] and equivalent directions, three 2-fold rotations around [1,0,0] and equivalent directions, and the identity. The MPG operations that leave Y invariant are the identity and the $\pm 120^\circ$ rotations around $[1, 1, -1]$, corresponding to point group 3. Likewise B, G, and R are left invariant by a conjugated point group, also with symbol 3 but with a different rotation axis. There are four such conjugated subgroups in the MPG 23, and the only common operation to all is the identity. Hence, the full CPG symbol is {23|3|1}. In this CPG, 3-fold rotations leave one color invariant and permute the other three, while 2-fold rotations exchange pairs of colors; for example, the 2-fold rotation around [1,0,0] exchanges Y with B and G with R.

The next step is to construct four "colored scalar" tensors of the selected rank using the projection method. This is done starting from the most generic form of the symmetric scalar tensor, to which we assign the color Y. We then apply the space transformation operations of the XPG and exchange the colors as explained in Sec. IV. We perform this operation for the lowest rank (rank 2), but the procedure is identical for any rank. The most generic rank-2 symmetric tensor is

$$\mathsf{T}_g = \begin{pmatrix} a & d & e \\ d & b & f \\ e & f & c \end{pmatrix}, \tag{4}$$

where the scalar quadratic form is obtained by multiplying this matrix to the left and right by $[k_x, k_y, k_z]$. The four colored

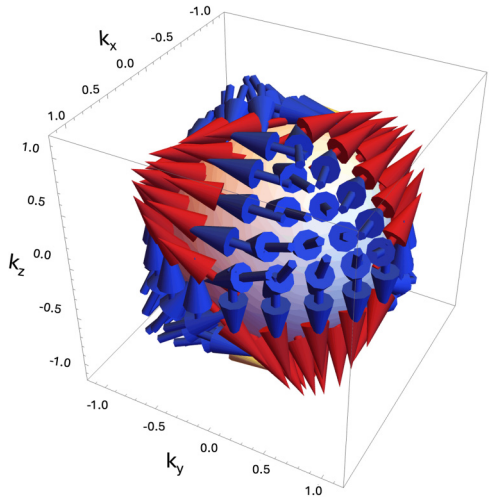

FIG. 2. Spin texture of $Mn_3Ir(Ge,Si)$, generated from the tensor in Eq. (7). The color of the arrows indicates the radial projection of the texture (red = out; blue = in). Wave vectors are in arbitrary units.

tensors obtained by the projection methods are

$$\mathsf{T}_Y = \frac{1}{12}\begin{pmatrix} A & B & -B \\ B & A & -B \\ -B & -B & A \end{pmatrix},$$

$$\mathsf{T}_B = \frac{1}{12}\begin{pmatrix} A & -B & B \\ -B & A & -B \\ B & -B & A \end{pmatrix},$$

$$\mathsf{T}_G = \frac{1}{12}\begin{pmatrix} A & -B & -B \\ -B & A & B \\ -B & B & A \end{pmatrix},$$

$$\mathsf{T}_R = \frac{1}{12}\begin{pmatrix} A & B & B \\ B & A & B \\ B & B & A \end{pmatrix}, \tag{5}$$

with $A = a + b + c$, $B = 1/2(d - e - f)$. With this construction, the set $\{\mathsf{T}_Y, \mathsf{T}_B, \mathsf{T}_G, \mathsf{T}_R\}$ is totally symmetric by the CPG; in other words, it is invariant by all geometrical transformations composed with the color permutation operations.

To obtain the spin texture at the lowest rank, we reassign colors to spin texture directions [Eq. (16)] and add up all the colored tensors, obtaining the full rank-3 CPG tensor

$$\mathsf{T}_{\rm CPG} = (1,1,-1)\mathsf{T}_Y + (1,-1,1)\mathsf{T}_B + (-1,1,1)\mathsf{T}_G + (-1,-1,-1)\mathsf{T}_R. \tag{6}$$

It is apparent that the texture obtained from Eq. (6) is completely invariant by rotation in spin space in the sense of Eq. (2). The expression of $\mathsf{T}_{\rm CPG}$ as a 3×6 matrix is

$$\mathsf{T}_{\rm CPG} = \begin{pmatrix} 0 & 0 & 0 & \Lambda_{14} & 0 & 0 \\ 0 & 0 & 0 & 0 & \Lambda_{14} & 0 \\ 0 & 0 & 0 & 0 & 0 & \Lambda_{14} \end{pmatrix}, \tag{7}$$

with $\Lambda_{14} = 1/3(-d + e + f)$ (see Fig. 2 for a depiction of the spin texture), and is formally identical to the one obtained from the MPG analysis, which is reported in Table I of Ref. [3] (MPG 23, Class XVII), exactly as we expected.

B. $Mn_3Ir(Ge, Si)$: 12-color analysis

We can repeat the same analysis using the experimental magnetic structure of $Mn_3Ir(Ge,Si)$, which requires twelve colors, none of which is left invariant by operations other than the identity; hence the 12-color CPG is $\{23|1|1\}$. Here, each of the four colors in the simplified magnetic structure is split into three, so that, for example,

$$\begin{aligned} &\text{Yellow 1 (Y1)} : \rightarrow (v_x, v_y, v_z), \\ &\text{Yellow 2 (Y2)} : \rightarrow (v_y, -v_z, -v_x), \\ &\text{Yellow 3 (Y3)} : \rightarrow (-v_z, v_x, -v_y), \end{aligned} \tag{8}$$

etc., where, in the experimental structure, $v_x = 0.7106$, $v_y = 1.2118$, $v_z = -1.015$. The analysis proceeds in the same way as for the 4-color structure, yielding the same result [Eq. (7)], this time with $\Lambda_{14} = 1/3(v_x f + v_y e + v_z d)$. Note the two results coincide for $\mathbf{v} = (1, 1, -1)$.

In conclusion, for $Mn_3Ir(Ge,Si)$, both the 4- and the 12-color analyses produce tensorial spin textures that are fully consistent with the MPG analysis (Ref. [3]), as we expected since the magnetic structure does not break any of the crystallographic symmetry operators. We generally expect this to be the case at every tensor order, whenever the "gray" (paramagnetic) group corresponding to the MPG is identical to the XPG. The CPG tensorial spin texture is formally invariant by a global rotation of the magnetic structure in spin space, and this remains true for spin orientations that break one or more of the MPG 23 symmetries. If such low-symmetry magnetic structure could be stabilized, we would expect the altermagneticlike component of the spin texture (given by the CPG analysis) to remain the same, while an additional component would be activated in the presence of SOC, with tensor forms consistent with the new, lower-symmetry MPG. However, to our knowledge, no such structure has been observed experimentally.

VI. DEALING WITH ANTICOLORS: THE CASE OF Pb_2MnO_4

Pb_2MnO_4 received some attention due to its potential multiferroic properties [27,28], and was recently discussed in Ref. [29] as having properties that are consistent with momentum-space spin splitting. It crystallizes with a tetragonal structure (space group: $P\bar{4}2_1c$) and orders noncollinearly at the Γ point below $\sim$18 K, with the magnetic moments on the eight Mn sites aligned along the diagonals of the square faces (Fig. 3). The MSG and MPG are $P\bar{4}'2_1c'$ and $\bar{4}'2m'$, respectively. As in the case of $Mn_3Ir(Ge,Si)$, magnetic ordering does not break any crystal symmetry operator, so we expect the CPG and MPG analyses (the latter reported in Table I of Ref. [3] as Class X) to yield identical results. However, the tensor associated with Class X has two parameters (Λ_{14} and Λ_{36}), so the specific values of these parameters in the CPG analysis will depend on the relative orientations of the spins in real space, while remaining invariant by global rotations in spin space.

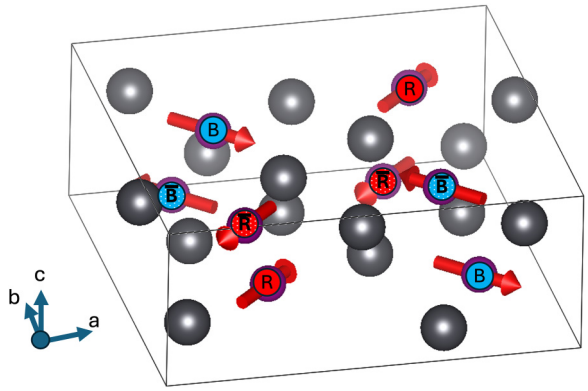

FIG. 3. Magnetic structure of Pb_2MnO_4, based on Ref. [27]. The magnetic Mn atoms have associated arrows, while the gray spheres are Pb (oxygen atoms have been omitted). Colors and anticolors are indicated with plain and dotted fields, respectively.

The colors/anticolors have been associated with magnetic moment directions, as follows:

$$\begin{aligned} \text{Red (R)} &: \rightarrow (1,1,0),\\ \text{Blue (B)} &: \rightarrow (1,-1,0),\\ \text{anti-Red } (\bar{\text{R}}) &: \rightarrow (-1,-1,0),\\ \text{anti-Blue } (\bar{\text{B}}) &: \rightarrow (-1,1,0). \end{aligned} \tag{9}$$

There are eight symmetry operators in the XPG: the identity (E), two $\bar{4}$ operations, a 2-fold rotation around z, two 2-fold axes along x and y, and two mirror planes perpendicular to xy and $\bar{x}y$. The corresponding color permutation operations are the following:

$$\begin{aligned} E &: \quad R\rightarrow R; B\rightarrow B; \bar{R}\rightarrow \bar{R}; \bar{B}\rightarrow \bar{B},\\ \bar{4}^{+} &: \quad R\rightarrow B; B\rightarrow \bar{R}; \bar{R}\rightarrow \bar{B}; \bar{B}\rightarrow R,\\ \bar{4}^{-} &: \quad R\rightarrow \bar{B}; B\rightarrow R; \bar{R}\rightarrow B; \bar{B}\rightarrow \bar{R},\\ 2_z &: \quad R\rightarrow \bar{R}; B\rightarrow \bar{B}; \bar{R}\rightarrow R; \bar{B}\rightarrow B,\\ 2_x &: \quad R\rightarrow \bar{B}; B\rightarrow \bar{R}; \bar{R}\rightarrow B; \bar{B}\rightarrow R,\\ 2_y &: \quad R\rightarrow B; B\rightarrow R; \bar{R}\rightarrow \bar{B}; \bar{B}\rightarrow \bar{R},\\ m_{xy} &: \quad R\rightarrow \bar{R}; B\rightarrow B; \bar{R}\rightarrow R; \bar{B}\rightarrow \bar{B},\\ m_{\bar{x}y} &: \quad R\rightarrow R; B\rightarrow \bar{B}; \bar{R}\rightarrow \bar{R}; \bar{B}\rightarrow B. \end{aligned} \tag{10}$$

Consequently, the H' subgroup (for red and antired) is $m = \{E, m_{\bar{x}y}\}$, while the group H only contains the identity. The CPG symbol is $\{\bar{4}2m|m|1\}$. The subgroup m has index 4 in $\bar{4}2m$, so $\{\bar{4}2m|m|1\}$ is a four-color group.

The four colored tensors obtained by the projection methods are

$$\mathsf{T}_R = \frac{1}{8}\begin{pmatrix} A & D & B\\ D & A & B\\ B & B & C\end{pmatrix},$$

$$\mathsf{T}_{\bar{R}} = \frac{1}{8}\begin{pmatrix} A & D & -B\\ D & A & -B\\ -B & -B & C\end{pmatrix},$$

$$\mathsf{T}_B = \frac{1}{8}\begin{pmatrix} A & -D & B\\ -D & A & -B\\ B & -B & C\end{pmatrix},$$

$$\mathsf{T}_{\bar{B}} = \frac{1}{8}\begin{pmatrix} A & -D & -B\\ -D & A & B\\ -B & B & C\end{pmatrix}, \tag{11}$$

with $A = a + b$, $B = (ee + f)/2$, $C = 2c$, and $D = d$. We can combine each color with its anticolor as

$$\mathsf{T}_{R-\bar{R}} = \frac{1}{4}\begin{pmatrix} 0 & 0 & B\\ 0 & 0 & B\\ B & B & 0\end{pmatrix},$$

$$\mathsf{T}_{B-\bar{B}} = \frac{1}{4}\begin{pmatrix} 0 & 0 & B\\ 0 & 0 & -B\\ B & -B & 0\end{pmatrix}. \tag{12}$$

Finally, we can reconstruct the full tensor using the color assignments in Eq. (9):

$$\mathsf{T}_{\text{CPG}} = \begin{pmatrix} 0 & 0 & 0 & \Lambda_{14} & 0 & 0\\ 0 & 0 & 0 & 0 & \Lambda_{14} & 0\\ 0 & 0 & 0 & 0 & 0 & 0\end{pmatrix}, \tag{13}$$

where $\Lambda_{14} = B$. This is to be compared with the MPG tensor for Class X:

$$\mathsf{T}_{\text{MPG}} = \begin{pmatrix} 0 & 0 & 0 & \Lambda_{14} & 0 & 0\\ 0 & 0 & 0 & 0 & \Lambda_{14} & 0\\ 0 & 0 & 0 & 0 & 0 & \Lambda_{36}\end{pmatrix}, \tag{14}$$

so T_{CPG} is a particular case of T_{MPG}, while $\Lambda_{36} = 0$ clearly arises from the fact that all magnetic moments are in the xy plane. One can easily verify that T_{CPG} is invariant by rotation in spin space in the sense of Eq. (2). It can also be shown that more general four-color models based on the same CPG produce an altermagneticlike tensor that is identical to T_{MPG}.

VII. BREAKING CRYSTAL SYMMETRY WITH MAGNETIC MOMENTS: THE CASE OF Mn_3GaN

The cases of $Mn_3Ir(Ge,Si)$ and Pb_2MnO_4 were complex and instructive, but mainly served as validations of the color symmetry approach, since there was an expectation that the results should coincide with the MPG analysis. Cases in which the crystal symmetry is explicitly broken by the magnetic structure are significantly more interesting, particularly when the phase diagram contains phases with different magnetic symmetries. The antiperovskite family, of which Mn_3GaN is a well-known representative [30,31], is an ideal case in point. In the bulk, Mn_3GaN orders with a noncollinear AFM structure and $T_N \sim 290$ K, but in thin films the Néel temperature can be as high as $T_N \sim 350$ K, making this material suitable for applications in spintronics. Since the magnetic Mn sites form kagome lattices with Ga at the empty sites, the magnetic ordering is in a typical 120° pattern, with the magnetic and crystallographic unit cells coinciding (Γ-point ordering). The crystallographic space group is $Pm\bar{3}m$ (No. 221). Two magnetic structures have been proposed for Mn_3GaN, corresponding to the Γ^{5g} and Γ^{4g} irreps of $Pm\bar{3}m$, and having MSGs $R\bar{3}m$ and $R\bar{3}m'$, respectively (see Fig. 4). Note that in both cases the cubic crystal symmetry is broken by the

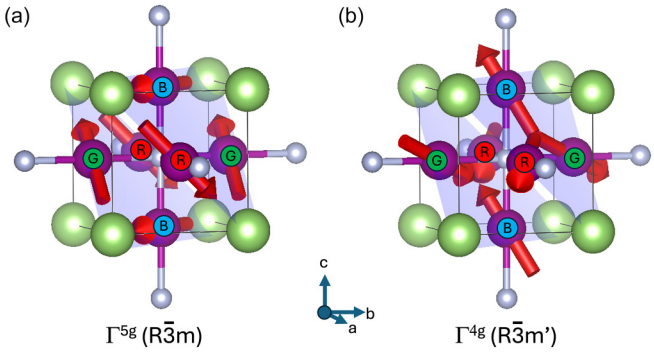

FIG. 4. Magnetic structures of the Γ^{5g} (a) and Γ^{4g} (b) phases of Mn_3GaN [30]. Magnetic Mn ions are shown with arrows, small spheres are N, and large spheres are Ga. (111) planes containing the Mn kagome lattice are shadowed.

magnetic structure. Mn_3GaN itself appears to be ordering with Γ^{5g} in both bulk [30] and thin film [32] forms, but DFT calculations [33] have shown that Γ^{4g} can be stable for other members of the antiperovskite family [34], sometimes associated with a Γ^{5g}/Γ^{4g} phase transition. As drawn in Fig. 4, the magnetic moments in the two structures are related by a 90° collective rotation of the magnetic moments in spin space. However, the MPG $\bar{3}m'$ of the Γ^{4g} is *admissible*; i.e., it allows the development of SOC-induced weak ferromagnetism via collective tilting of the moments toward the [1,1,1] direction.

A. Mn_3GaN: CPG analysis

The XPG $m\bar{3}m$ comprises 48 symmetry operations, but improper operations have the same effect on magnetic moments as the corresponding proper rotations, so it will be sufficient to consider the 24 operations of point group 432: eight 3-fold (±120°) rotations, around [1,1,1] and equivalent directions, three 2-fold rotations and six 4-fold rotations around [1,0,0] and equivalent, six 2-fold rotations around [1,1,0] equivalent, and the identity. The color assignment (shown in Fig. 4) is the same for the Γ^{5g} and Γ^{4g} structures, except for a collective rotation in spin space. For Γ^{5g},

$$\begin{aligned} \mathrm{R}^{5g} &: \to \tfrac{1}{\sqrt{2}}\,(0,1,-1),\\ \mathrm{B}^{5g} &: \to \tfrac{1}{\sqrt{2}}\,(1,-1,0),\\ \mathrm{G}^{5g} &: \to \tfrac{1}{\sqrt{2}}\,(-1,0,1), \end{aligned} \tag{15}$$

while for Γ^{4g},

$$\begin{aligned} \mathrm{R}^{4g} &: \to \tfrac{1}{\sqrt{6}}\,(-2,1,1),\\ \mathrm{B}^{4g} &: \to \tfrac{1}{\sqrt{6}}\,(1,1,-2),\\ \mathrm{G}^{4g} &: \to \tfrac{1}{\sqrt{6}}\,(1,-2,1). \end{aligned} \tag{16}$$

By inspection, the 3-fold rotations permute the three colors, the [1,0,0]-2-fold rotations leave all colors invariant, while the [1,0,0]-4-fold rotations and [1,1,0]-2-fold rotations leave one color invariant and permute the other two. Hence, the color group symbol is {432|422|222}. The point group 422 is a subgroup of index three, so {432|422|222} is indeed a three-color group.

Next, we construct the colored tensors with the projection method, starting from a generic rank-2 tensor [Eq. (4)] and, this time, assigning the color red (R) to it:

$$\mathsf{T}_R = \frac{1}{6}\begin{pmatrix} 2a & 0 & 0\\ 0 & b+c & 0\\ 0 & 0 & b+c \end{pmatrix},$$

$$\mathsf{T}_B = \frac{1}{6}\begin{pmatrix} b+c & 0 & 0\\ 0 & b+c & 0\\ 0 & 0 & 2a \end{pmatrix},$$

$$\mathsf{T}_G = \frac{1}{6}\begin{pmatrix} b+c & 0 & 0\\ 0 & 2a & 0\\ 0 & 0 & b+c \end{pmatrix}.$$

Reassembling the full CPG tensor we obtain, for Γ^{5g},

$$\mathsf{T}^{5g}_{\mathrm{CPG}} = \Lambda\begin{pmatrix} 0 & 1 & -1 & 0 & 0 & 0\\ -1 & 0 & 1 & 0 & 0 & 0\\ 1 & -1 & 0 & 0 & 0 & 0 \end{pmatrix} \tag{17}$$

with $\Lambda = -(1/6\sqrt{2})(2a-b-c)$, while for Γ^{4g},

$$\mathsf{T}^{4g}_{\mathrm{CPG}} = \Lambda\begin{pmatrix} 2 & -1 & -1 & 0 & 0 & 0\\ -1 & 2 & -1 & 0 & 0 & 0\\ -1 & -1 & 2 & 0 & 0 & 0 \end{pmatrix} \tag{18}$$

with $\Lambda = -(1/6\sqrt{6})(2a-b-c)$.

The two tensors are orthogonal, meaning that the spin textures will be orthogonal at any wave vector.

As already explained, the MPGs for the Γ^{5g} and Γ^{4g} ($\bar{3}m$ and $\bar{3}m'$, Class VIII and Class VII, respectively in Table I of Ref. [3]) belong to the trigonal system. Therefore, in order to compare them to the CPG tensors, we need to rotate them to the cubic coordinates. The simple transformations yield

$$\begin{aligned} \mathsf{T}^{\bar{3}m} = {}& \Lambda_1\begin{pmatrix} 0 & 1 & -1 & 0 & 0 & 0\\ -1 & 0 & 1 & 0 & 0 & 0\\ 1 & -1 & 0 & 0 & 0 & 0 \end{pmatrix}\\ & + \Lambda_2\begin{pmatrix} 0 & 0 & 0 & 0 & 1 & -1\\ 0 & 0 & 0 & -1 & 0 & 1\\ 0 & 0 & 0 & 1 & -1 & 0 \end{pmatrix}, \end{aligned} \tag{19}$$

$$\begin{aligned} \mathsf{T}^{\bar{3}m'} = {}& \Lambda_1\begin{pmatrix} 2 & -1 & -1 & 0 & 0 & 0\\ -1 & 2 & -1 & 0 & 0 & 0\\ -1 & -1 & 2 & 0 & 0 & 0 \end{pmatrix}\\ & + \Lambda_2\begin{pmatrix} 0 & 0 & 0 & 2 & -1 & -1\\ 0 & 0 & 0 & -1 & 2 & -1\\ 0 & 0 & 0 & -1 & -1 & 2 \end{pmatrix}\\ & + \Lambda_3\begin{pmatrix} 1 & 1 & 1 & 0 & 0 & 0\\ 1 & 1 & 1 & 0 & 0 & 0\\ 1 & 1 & 1 & 0 & 0 & 0 \end{pmatrix}. \end{aligned} \tag{20}$$

One can easily see that $\mathsf{T}^{5g}_{\mathrm{CPG}}$ [Eq. (17)] is equal to the first term of $\mathsf{T}^{\bar{3}m}$ [Eq. (19)] with $\Lambda \to \Lambda_1$. Likewise, $\mathsf{T}^{4g}_{\mathrm{CPG}}$ [Eq. (18)] is equal to the first term of $\mathsf{T}^{\bar{3}m'}$ [Eq. (20)] with $\Lambda \to \Lambda_1$. In other words, tensors obtained from the CPG analysis are special cases of the general tensors allowed by the MPG, obtained, in this case, by setting $\Lambda_2 = \Lambda_3 = 0$. This is exactly what we expected and is completely consistent with the result we previously obtained for collinear structures (Ref. [3]).

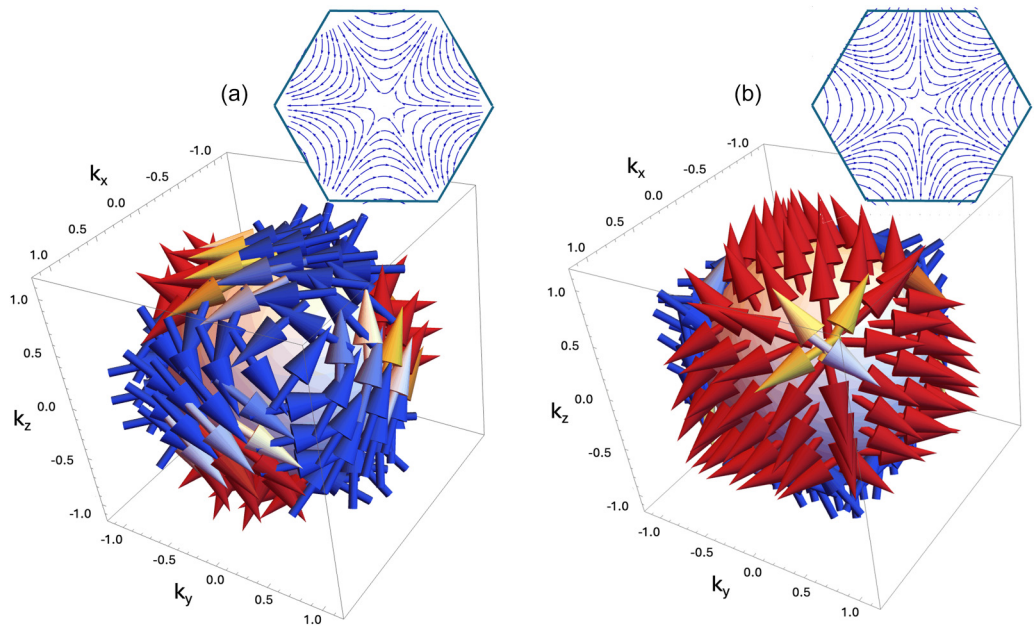

FIG. 5. Altermagneticlike spin textures for the Γ^{5g} (a), Γ^{4g} (b), and phases of Mn_3GaN, generated from the tensors $\mathsf{T}^{5g}_{\mathrm{CPG}}$ and $\mathsf{T}^{4g}_{\mathrm{CPG}}$ [Eqs. (17) and (18)]. The color of the arrows indicates the radial projection of the texture (red = out; yellow/gray = parallel; blue = in). Wave vectors are in arbitrary units. The insets are the equatorial cross sections of the textures down the (1,1,1) direction, shown with an outline of the Brillouin zone (compare with Fig. 6). The Γ^{5g} and Γ^{4g} textures are related by a collective 90° rotation in spin space around the (1,1,1) direction.

B. Mn_3GaN and $Mn_3Ir(Ge,Si)$: SG analysis

Here, we give examples of analyses performed on Mn_3GaN and $Mn_3Ir(Ge,Si)$ with the SG approach and using the terminology and numbering of Ref. [23]. As already mentioned, the SGs corresponding to a given CPG are obtained from the XPG $G(R)$ and one of its normal subgroups $H(r)$, where the letter in parentheses corresponds to the notation of Ref. [23].

In the case of Mn_3GaN, $G = 432$ and $H = 222$. The spin group is constructed by selecting spin-transformation PGs (denoted as B) that are isomorphic to G/H (or R/r in the notation of Ref. [23]). There are two possible PGs for B: 32 (SG No. 563) and $3m$ (SG No. 564), which are, indeed, both isomorphic to the three-color permutation group. In Ref. [23], it is explained that the two coordinate systems for G and B are arbitrarily mutually orientated, though a complex notation is introduced when the coordinate systems of B and G do not coincide. However, importantly, one needs to orient the axes of B so that they act correctly on the spin system in real space. In our case, the 3-fold axis must be perpendicular to the three spins, each 2-fold axis in 32 must be parallel to one of the spins, and each mirror plane in $3m$ must be perpendicular to one of the spins. When this is done, the analysis is identical to the one using CPGs, since B acts by permuting the spins in the same way as colors were permuted by the CPG. Note, however, that the B needs to be rotated by 90° between Γ^{5g} and Γ^{4g} and more generally reoriented to fit an arbitrary rotation in spin space. Leaving aside the $32/3m$ ambiguity, this seems an unnecessary complication that is completely avoided by the CPG analysis. Within the tensorial framework, the CPG analysis also captures the fundamentally *scalar* nature of altermagneticlike tensors.

Similarly, a parallel SG analysis can be performed on $Mn_3Ir(Ge,Si)$, where $G = 23$ and $H = 1$ (SG 538 in Ref. [23]). Here, the SG is the *same* for the approximate and experimental magnetic structures (see Secs. V and V B), while the CPGs are different—{23|3|1} vs {23|1|1}—because, as already explained, the CPG symbol encodes additional information about the number of colors (i.e., distinct spin directions) and the specific representation that encodes the color permutation.

C. Mn_3GaN: DFT calculations and tensor decompositions

To validate our analysis further, we calculated the spin textures for the Γ^{5g} and Γ^{4g} phases of Mn_3GaN using spin-resolved DFT. DFT calculations were performed using the Quantum-ESPRESSO code [35]. The exchange and correlation effects were treated within the generalized gradient approximation (GGA) [36]. The k-point mesh of $16 \times 16 \times 16$ and plane-wave cutoff energy of 52 Ry were used for the integration in the irreducible Brillouin zone. The noncollinear magnetic structure was always considered with and without spin-orbit coupling. The spin texture on the Fermi surface was calculated using $50 \times 50 \times 50$ k points within the first Brillouin zone (BZ). To depict the results in an intuitive manner, the spin texture was projected on a plane containing the Γ point and normal to the (1,1,1) direction.

Figure 6 displays equatorial sections [i.e., on a plane cut perpendicularly to the (1, 1, 1) direction] of the spin-resolved Fermi surface, calculated for Γ^{5g} and Γ^{4g} with and without SOC. For Γ^{4g}, the color wheel indicating in-plane spin directions was rotated by 90°, to emphasise the expected relation with the Γ^{5g} texture. Band dispersions along high-symmetry directions are displayed in Figs. S2 and S3 of the

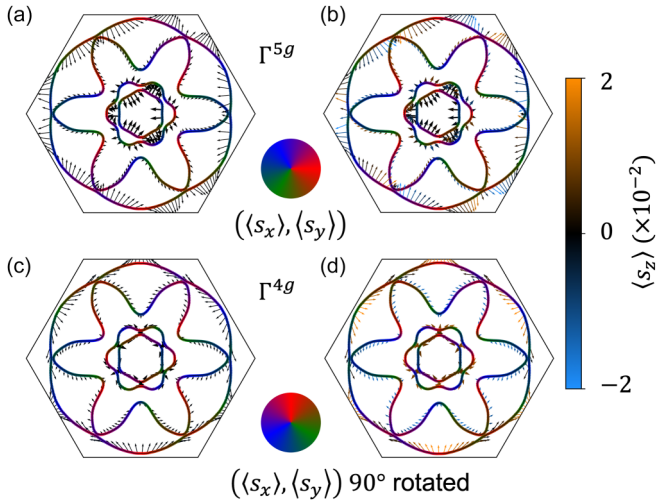

FIG. 6. Spin texture at the Fermi surface on a plane cut perpendicularly to the (1,1,1) direction including the Γ point shown with an outline of the BZ, calculated using spin-resolved DFT for the Γ^{5g} (top) and Γ^{4g} (bottom) phases with [(a), (c)] and without [(b), (d)] SOC. For Γ^{4g}, the color wheel indicating in-plane spin directions was rotated by 90°. The z component, which is only present with SOC, is also indicated. For Γ^{4g}, each band has a net magnetization. The z direction is along (1,1,1).

Supplemental Material [37]. In the absence of SOC, the Γ^{5g} [panel (a)] and Γ^{4g} [panel (c)] are identical except for the 90° rotation, and there is no spin-texture component along (1,1,1), as predicted by the CPG analysis at any tensor rank. The spin textures are also very similar to those in Fig. 5 (see insets for the same cuts). By contrast, in the presence of SOC, the Γ^{5g} [panel (b)] and Γ^{4g} [panel (d)] become significantly different, and acquire a component along (1,1,1). In the case of Γ^{5g}, this component arises from a higher-rank tensor (see below) and averages to zero for each band, while for Γ^{4g} the additional Λ_3 term [Eq. (20)] yields a net spin polarization in each band, and an overall weak magnetization for the whole structure.

To demonstrate the effectiveness of our tensorial approach, we fitted the spin textures from DFT onto tensorial expansions based on CPG (no SOC) and MPG (with SOC) analyses for both Γ^{4g} and Γ^{5g}. To this end, we decomposed the spin textures of the equatorial sections [i.e., sections perpendicular to (111), as in Fig. 6] for the four bands that cross the Fermi surface into a *radial* component perpendicular to **k** and to (111), a *tangential* component in the equatorial plane and perpendicular to **k**, and an *axial* component parallel to (111), which is zero in the absence of SOC. (The bands are labeled from 0 to 3 as we move away from the Γ point as shown in the SM [37], Fig. S4.) Note that, with DFT, the spin texture is calculated on constant-energy surfaces rather than at constant $|\mathbf{k}|$. However, since constant-energy surfaces have at least the full symmetry of the XPG, textures will have an identical tensorial expansion, though the coefficients will be different. CPG tensor decompositions were performed up to tensorial rank 18, while MPG decompositions of the axial component were to rank 13 (we recall that MPG tensors are odd ranked, while CPG tensors are even ranked). The three tensorial components of the spin texture are linear combinations of sine and cosine functions of the azimuthal angle ϕ in the equatorial plane. The coefficients of this expansion (four for the radial and tangential components, three for the axial component) were fitted to the corresponding components of the DFT spin textures. The results of these fits are displayed graphically in Fig. 7 for band 1. Corresponding representations for the other bands are in Figs. S5–S7 of the SM [37], while the functional form and fitted parameters are displayed in Tables S1 and S2 of the SM.

In the absence of SOC, the radial and tangential components are swapped between Γ^{5g} and Γ^{4g}, while the axial component is absent. This is completely consistent with the CG analysis, and, in particular, with the fact that textures for Γ^{5g} and Γ^{4g} are rotated by 90° in spin space. When SOC is switched on, a small axial component (approximately a factor of 10 smaller) appears for both Γ^{5g} and Γ^{4g}. However, for Γ^{5g} the axial spin polarization averaged over the Fermi surface is zero, while for Γ^{4g} there is a net spin polarization, consistent with weak ferromagnetism. Further details of the effects of SOC on the spin-polarized band structures are evident from the band dispersions in Figs. S2 and S3 of the SM [37]. Particularly noteworthy is the fact that the bands along the Γ-*R* direction must, by symmetry, have polarization along the (111) direction. Hence, a small band splitting is observed only for Γ^{4g} in the presence of SOC, where the band remains unsplit in all other cases (see insets).

VIII. DISCUSSION AND CONCLUSIONS

In this paper, "altermagneticlike" spin textures have been defined as the components of the momentum-space spin texture that is invariant by global rotations in spin space in the sense of Eq. (2). The tensorial forms of these textures can be defined consistently based on CPG analysis for both noncollinear and collinear AFM structures, since the latter are a special example of bicolor (black and white) symmetry. Strong FM textures (i.e., those present in a true ferro/ferrimagnet rather than a weak/canted FM) are also a special example, for which the color group is trivial (colorless) [38]. In addition to altermagneticlike textures, the MPG of the crystal/magnetic structure will generally allow additional ("nonaltermagnetic") spin textures in momentum space, which will be specific to a given orientation of the spin system and will be absent in the absence of SOC. Altermagneticlike/ferromagnetic textures are allowed at some tensorial order for all MPGs that do not explicitly forbid $\mathbf{k}/-\mathbf{k}$-*symmetric*, time-reversal odd spin textures (i.e., those that do not contain the time-reversal operator or the product of inversion and time-reversal operators). The MPG/CPG pair defines which part of the full MPG texture (tabulated to lowest tensorial order in Ref. [3]) is altermagneticlike, with the CPG also providing the "tensorial building blocks" (colored tensors) to reconstruct the full altermagneticlike texture, once the exact real-space spin orientations are defined. These building blocks can in principle be derived for all CPGs once and for all, though calculating them for a specific magnetic structure is a simple exercise. We have demonstrated the CPG approach for three noncollinear magnetic structures: $Mn_3Ir(Ge,Si)$, Pb_2MnO_4, and Mn_3GaN. In the case of Mn_3GaN, using DFT we have also calculated the spin

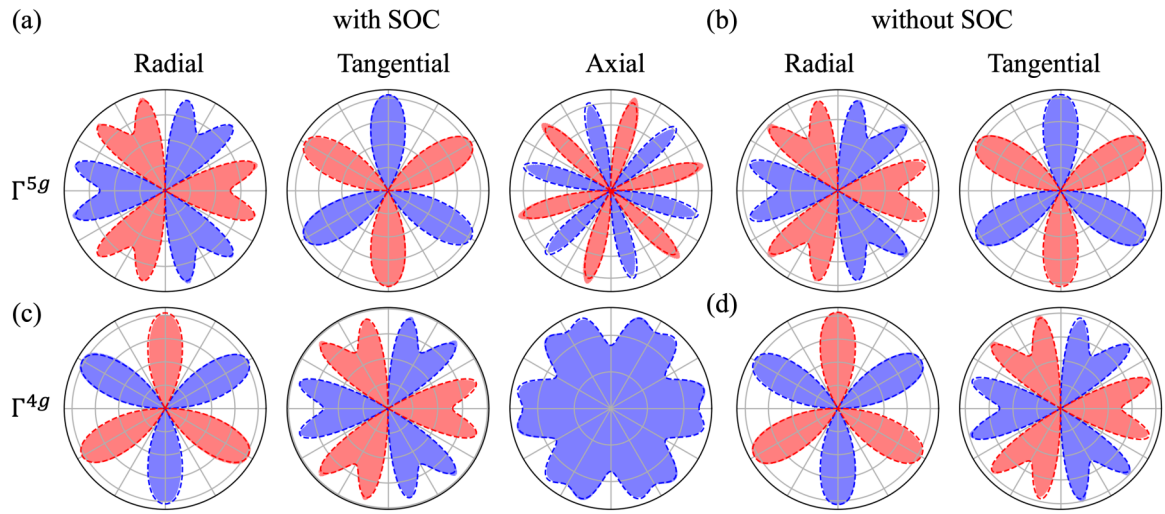

FIG. 7. Decomposition of the band-1 spin textures calculated with DFT (solid blocks) and with the corresponding tensorial fits (dashed lines) for Γ^{5g} (top row) and Γ^{4g} (bottom row). Red/blue indicate positive/negative components (note the $\mathbf{k}/-\mathbf{k}$ symmetry). Panels (a)/(c) and (b)/(d) were calculated respectively with and without SOC (see text). The outer circles in the plots correspond to amplitudes for the radial, tangential, and axial components of [0.190,0.208,0.009]/[0.205,0.190,0.013] or (0.198,0.208)/(0.208,0.198) for the Γ^{5g}/Γ^{4g} phase, respectively, with [ ] or without ( ) SOC, respectively.

textures for two different magnetic phases (Γ^{5g} and Γ^{4g}) with and without SOC, and demonstrated that they are entirely consistent with the predictions of MPG/CPG theory. We also find that the tensorial decomposition of the DFT textures is in very good agreement with CPG (no SOC) and MPG (with SOC) predictions, confirming the soundness of this method.

Beyond the results reported in this paper, we remark that CPG/CSG symmetry can also be defined for *p*-wave magnets [5] and other systems (e.g., based on triangular lattices) [6], which allow $\mathbf{k}/-\mathbf{k}$-*antisymmetric*, time-reversal even spin textures in momentum space, and it is expected that those spin textures will also be constrained by CSG symmetry. However, our tensorial analysis will need to be modified to deal with such systems [39].

ACKNOWLEDGMENTS

The authors would like to acknowledge the use of the University of Oxford Advanced Research Computing (ARC) facility [40] in carrying out this work.

DATA AVAILABILITY

The data that support the findings of this article are openly available [41].

APPENDIX: COLOR SYMMETRY, REPRESENTATIONS, AND EXCHANGE MULTIPLETS

There is a close relation between the description of magnetic structures in terms of CGs and the theory of exchange multiplets [22], which classifies magnetic structures in terms of irreducible representations (*irreps*) of the symmetry group of a Hamiltonian that only involves symmetric exchange and is therefore invariant by rotation in spin space. The symmetry of this Hamiltonian is higher than the crystal symmetry; thus, in general, several irreps of the space group will be combined into so-called "exchange multiplets" and may be activated simultaneously at a magnetic phase transition. Exchange multiplets are constructed as tensor products of a single irrep of the space group that is contained in the full permutational (scalar) representation of the equivalent magnetic sites (with dimensionality equal to the number of sites), times the (generally reducible) axial-vector representation (see Ref. [22]).

By contrast, the set of all possible magnetic structures with a given CG and for a given set of equivalent magnetic sites is constructed as the tensor product of the "color-permuting representation" times the axial-vector representation. In turn, the color-permuting representation is the permutational representation of the magnetic sites restricted to the subspace defined by a one-color basis set, where all the sites with a given color are assigned the number 1, while all the other sites are assigned 0. This basis set can be easily constructed projectively from the one-site basis of the permutational representation. This is done from the left-coset decomposition of H' in G:

$$G = H' + g_1 \circ H' + g_2 \circ H' + \cdots . \tag{A1}$$

Let $\boldsymbol{b}$ be an element of the one-site basis set of the permutational representation of the magnetic sites, such that one of the sites is associated with the number 1 and all the others with 0. Let $h'_i,\ i = 1, \ldots, n$, be all the elements of H'. Then the elements of the one-color basis set, say $\boldsymbol{b}_R, \boldsymbol{b}_Y, \boldsymbol{b}_G$, etc., are defined as

$$\begin{aligned} \boldsymbol{b}_R &= \frac{1}{n}\sum_{i=1}^{n} h'_i[\boldsymbol{b}], \\ \boldsymbol{b}_Y &= \frac{1}{n}\sum_{i=1}^{n} g_1 \circ h'_i[\boldsymbol{b}], \\ \boldsymbol{b}_G &= \frac{1}{n}\sum_{i=1}^{n} g_2 \circ h'_i[\boldsymbol{b}], \\ &\cdots . \end{aligned} \tag{A2}$$

One can easily see that this basis is in accord with the definition of the CGs, whereby "red" sites are those where $\boldsymbol{b}_R$ is nonzero, etc. H' brings red sites into red sites, $g_1 \circ H'$ brings red sites into yellow sites, etc. The CG also defines the representation of G onto the linear space defined by the one-color basis set, since the transformation matrices can be written out explicitly.

A basis set for the linear space of all magnetic structures with a given color group is

$$(\boldsymbol{b}_R\hat{\mathbf{i}}, \boldsymbol{b}_R\hat{\mathbf{j}}, \boldsymbol{b}_R\hat{\mathbf{k}}, \boldsymbol{b}_Y\hat{\mathbf{i}}, \boldsymbol{b}_Y\hat{\mathbf{j}}, \boldsymbol{b}_Y\hat{\mathbf{k}}, \boldsymbol{b}_G\hat{\mathbf{i}}, \boldsymbol{b}_G\hat{\mathbf{j}}, \boldsymbol{b}_G\hat{\mathbf{k}}, \dots). \tag{A3}$$

The generic elements of this linear space are

$$\boldsymbol{b}_R\,\mathbf{v}_1 + \boldsymbol{b}_Y\,\mathbf{v}_2 + \boldsymbol{b}_G\,\mathbf{v}_3 + \cdots, \tag{A4}$$

where $\mathbf{v}_1$, $\mathbf{v}_2$, etc., are generic linear combinations of the unit vectors $\hat{\mathbf{i}}$, $\hat{\mathbf{j}}$, and $\hat{\mathbf{k}}$. This corresponds to assigning a generic vector to each of the colors, exactly as we anticipated.

Finally, since the color-permuting representation, with dimensionality equal to the number of colors, is generally *reducible*, it follows that each CG describes several exchange multiplets.

[1] L. Šmejkal, J. Sinova, and T. Jungwirth, Beyond conventional ferromagnetism and antiferromagnetism: A phase with nonrelativistic spin and crystal rotation symmetry, Phys. Rev. X **12**, 031042 (2022).

[2] L. Šmejkal, J. Sinova, and T. Jungwirth, Emerging research landscape of altermagnetism, Phys. Rev. X **12**, 040501 (2022).

[3] P. G. Radaelli, Tensorial approach to altermagnetism, Phys. Rev. B **110**, 214428 (2024).

[4] S. W. Cheong and F. T. Huang, Altermagnetism with noncollinear spins, npj Quantum Mater. **9**, 13 (2024).

[5] A. B. Hellenes, T. Jungwirth, R. Jaeschke-Ubiergo, A. Chakraborty, J. Sinova, and L. Šmejkal, *p*-wave magnets, arXiv:2309.01607.

[6] S. Hayami, Y. Yanagi, and H. Kusunose, Spontaneous antisymmetric spin splitting in noncollinear antiferromagnets without spin-orbit coupling, Phys. Rev. B **101**, 220403(R) (2020).

[7] Here "$\mathbf{k}/-\mathbf{k}$*symmetric/antisymmetric*" means that the spin texture, defined as $\mathbf{s}_{n\mathbf{k}} = \langle\Psi_{n\mathbf{k}}|\boldsymbol{\sigma}|\Psi_{n\mathbf{k}}\rangle$ (see below), is the same/changes sign by exchanging $\mathbf{k}$ and $-\mathbf{k}$. "Time-reversal odd/even" means that the spin texture in the time-reversed magnetic domain (i.e., the domain obtained by flipping all the magnetic moments) is opposite/the same for a given $\mathbf{k}$.

[8] G. Dresselhaus, Spin-orbit coupling effects in zinc blende structures, Phys. Rev. **100**, 580 (1955).

[9] E. I. Rashba and V. I. Sheka, Symmetry of energy bands in crystals of Wurtzite type II. Symmetry of bands with spin-orbit interaction included, Fiz. Tverd. Tela: Collected Papers **2**, 62 (1959) [New. J. Phys. **17**, 050202 (2015)].

[10] J. Železný, Y. Zhang, C. Felser, and B. Yan, Spin-polarized current in noncollinear antiferromagnets, Phys. Rev. Lett. **119**, 187204 (2017).

[11] J. Sticht, K. H. Höck, and J. Kübler, Non-collinear itinerant magnetism: The case of Mn_3Sn, J. Phys.: Condens. Matter **1**, 8155 (1989).

[12] As explained in the remainder, the CG approach can be employed to describe the magnetic structures of $\mathbf{k}/-\mathbf{k}$-antisymmetric magnets, but colored tensors as defined here would require some modifications. For this reason, we will exclude $\mathbf{k}/-\mathbf{k}$-antisymmetric magnets from our treatment.

[13] B. Brekke, P. Sukhachov, H. G. Giil, A. Brataas, and J. Linder, Minimal models and transport properties of unconventional *p*-wave magnets, Phys. Rev. Lett. **133**, 236703 (2024).

[14] D. Harker, The three-colored three-dimensional space groups, Acta Crystallogr. Sect. A **37**, 286 (1981).

[15] J. Sivardière, Sous-groupes des groupes d'espace et groupes à trois couleurs, Acta Crystallogr. Sect. A **40**, 573 (1984).

[16] R. L. Roth, Coloring $p4m$ with two, four, and six colors, Acta Crystallogr. Sect. A **41**, 484 (1985).

[17] J. Sivardière, Groupes d'espace à quatre et six couleurs, Acta Crystallogr. **44**, 735 (1988).

[18] J. N. Kotzev and D. A. Alexandrova, Full tables of colour space groups with colour-preserving translations, Acta Crystallogr. Sect. A **44**, 1082 (1988).

[19] D. B. Litvin, J. N. Kotzev, and J. L. Birman, Physical applications of crystallographic color groups: Landau theory of phase transitions, Phys. Rev. B **26**, 6947 (1982).

[20] Z. Jirák, Group-theoretical approach to orbital ordering in crystals with E_g and T_{2g} ions, Phys. Rev. B **46**, 8725 (1992).

[21] E. F. Bertaut, Representation analysis of magnetic structures, Acta Crystallogr. Sect. A **24**, 217 (1968).

[22] Y. A. Izyumov, Exchange multiplets in the theory of magnetic structures of crystals, J. Magn. Magn. Mater. **15-18**, 497 (1980).

[23] D. B. Litvin, Spin point groups, Acta Crystallogr. Sect. A **33**, 279 (1977).

[24] T. Eriksson, L. Bergqvist, P. Nordblad, O. Eriksson, and Y. Andersson, Structural and magnetic characterization of Mn_3IrGe and $Mn_3Ir(Si_{1-x}Ge_x)$: Experiments and theory, J. Solid State Chem. **177**, 4058 (2004).

[25] T. Eriksson, R. Lizárraga, S. Felton, L. Bergqvist, Y. Andersson, P. Nordblad, and O. Eriksson, Crystal and magnetic structure of Mn_3IrSi, Phys. Rev. B **69**, 054422 (2004).

[26] M. Hu, O. Janson, C. Felser, P. McClarty, J. van den Brink, and M. G. Vergniory, Spin Hall and Edelstein effects in novel chiral noncollinear altermagnets, arXiv:2410.17993.

[27] S. A. Kimber and J. P. Attfield, Magnetic order in acentric Pb_2MnO_4, J. Mater. Chem. **17**, 4885 (2007).

[28] D. C. Kakarla, H. C. Wu, D. J. Hsieh, P. J. Sun, G. J. Dai, J. Y. Lin, J. L. Her, Y. H. Matsuda, L. Z. Deng, M. Gooch, C. W. Chu, and H. D. Yang, Metamagnetic transitions and magnetoelectric coupling in acentric and nonpolar Pb_2MnO_4, Phys. Rev. B **99**, 195129 (2019).

[29] S.-W. Cheong and F.-T. Huang, Kinetomagnetism and altermagnetism, arXiv:2503.16277.

[30] E. F. Bertaut, D. Fruchart, J. P. Bouchaud, and R. Fruchart, Diffraction neutronique de Mn_3GaN, Solid State Commun. **6**, 251 (1968).

[31] K. Shi, Y. Sun, J. Yan, S. Deng, L. Wang, H. Wu, P. Hu, H. Lu, M. I. Malik, Q. Huang, and C. Wang, Baromagnetic effect in antiperovskite $Mn_3Ga_{0.95}N_{0.94}$ by neutron powder diffraction analysis, Adv. Mater. **28**, 3761 (2016).

[32] T. Nan, C. X. Quintela, J. Irwin, G. Gurung, D. F. Shao, J. Gibbons, N. Campbell, K. Song, S. Y. Choi, L. Guo, R. D. Johnson, P. Manuel, R. V. Chopdekar, I. Hallsteinsen, T. Tybell, P. J. Ryan, J. W. Kim, Y. Choi, P. G. Radaelli, D. C. Ralph *et al.*, Controlling spin current polarization through non-collinear antiferromagnetism, Nat. Commun. **11**, 4671 (2020).

[33] H. K. Singh, I. Samathrakis, N. M. Fortunato, J. Zemen, C. Shen, O. Gutfleisch, and H. Zhang, Multifunctional antiperovskites driven by strong magnetostructural coupling, npj Comput. Mater. **7**, 98 (2021).

[34] Note that the Γ^{4g} magnetic structure is the same as for the compound Mn_3Ir reported in Ref. [10]. The schematic spin texture reported in their Fig. 3 is very similar to the one we calculate here.

[35] P. Giannozzi, O. Andreussi, T. Brumme, O. Bunau, M. Buongiorno Nardelli, M. Calandra, R. Car, C. Cavazzoni, D. Ceresoli, M. Cococcioni, N. Colonna, I. Carnimeo, A. Dal Corso, S. De Gironcoli, P. Delugas, R. A. Distasio, A. Ferretti, A. Floris, G. Fratesi, G. Fugallo *et al.*, Advanced capabilities for materials modelling with Quantum ESPRESSO, J. Phys.: Condens. Matter **29**, 465901 (2017).

[36] J. P. Perdew, K. Burke, and M. Ernzerhof, Generalized gradient approximation made simple, Phys. Rev. Lett. **77**, 3865 (1996).

[37] See Supplemental Material at http://link.aps.org/supplemental/10.1103/r34k-xjpx for I. Further discussion of the relation between color groups and spin groups; II. Spin-resolved band dispersions of Mn_3GaN; III. Fermi surfaces of Mn_3GaN; IV. Decompositions of the Fermi surfaces (Bands 0, 2, 3) spin textures of Mn_3GaN onto tensorial expansions.

[38] Note that the net magnetization in the absence of SOC is *identically zero* for collinear altermagnets and also for noncollinear magnets where each color has a corresponding anticolor, since the magnetization of anticolored sublattices cancels.

[39] Very briefly, magnets with $\mathbf{k}/-\mathbf{k}$ *antisymmetric* splitting are characterized by bond-type multipolar ordering [6], and the staggered magnetization (in the collinear case) or the one-color axial unit vectors (noncollinear case) need to be replaced in the tensorial treatment by the cross product $\boldsymbol{S}_1 \times \boldsymbol{S}_2$, where sites 1 and 2 are those connected by the specific bond. This approach will be fully described in a future paper.

[40] A. Richards, University of Oxford Advanced Research Computing, Zenodo (2015), see https://doi.org/10.5281/zenodo.22558.

[41] P. Radaelli and G. Gurung, Data linked to the publication "Color symmetry and altermagneticlike spin textures in noncollinear antiferromagnets" (University of Oxford, 2025), see https://dx.doi.org/10.5287/ora-ng7pyddap.